AJNR

Dyke Postmortem CT and Award. autopsy in perinatal intracranial hemorrhage.

B Ludwig, K Becker, G Rutter, J Bohl and M Brand

AJNR Am J Neuroradiol 1983, 4 (1) 27-36
http://www.ajnr.org/content/4/1/27

This information is current as of August 11, 2025.

Dyke Award

Postmortem CT and Autopsy in Perinatal Intracranial Hemorrhage

B. Ludwig[1]
K. Becker[2]
G. Rutter[2]
J. Bohl[3]
M. Brand[4]

To improve interpretation of intracranial computed tomographic findings in vivo, postmortem computed tomography was correlated directly with autopsy findings in 105 specimens of human stillborn and live-birth infants, ranging in age from gestational week 13 to postnatal month 18. This study identifies the typical computed tomographic appearance of intradural and other hemorrhages, attempts to correlate the type of hemorrhage with brain maturity, and documents that postmortem computed tomography is useful to the neuropathologist as a supplementary method complementing the traditional postmortem examination.

In recent years, computed tomography (CT) and sonography of newborns have greatly improved our understanding of neonatal intracranial hemorrhage [1–10]. New insights into in vivo morphology combined with large follow-up studies [11–15] have made it possible to predict the survivor's outcome. Although quality control of a morphologic diagnostic procedure such as CT depends ultimately on pathologic confirmation of its accuracy, there has been very little direct correlation of CT and postmortem pathology [16–20].

Postmortem CT provides a unique method of assessing the reliability of CT for detecting and characterizing intracranial pathology. It has specific advantages: (1) CT findings and pathology can be directly correlated because there is no progression of pathology in the highly variable interval between the last in vivo CT study and the postmortem examination. (2) CT provides immediate information about the state of the brain at postmortem, unlike the traditional study, which requires delay for proper brain fixation prior to cutting. (3) If autopsy is refused, CT can be used to determine intracranial changes in the individual case and add to information about these changes in the patient population. (4) If autopsy is handicapped by advanced maceration, sufficient information about brain morphology can still be expected from CT. (5) Information gained by postmortem CT can influence the way in which the pathologic specimen is examined. By comparing axial CT cuts with horizontal brain sections, for example, the pathologist benefits in discovering small details like subependymal hematomas, or in marking off areas with slight density deviations on CT. (6) The space-occupying effect of intracranial hemorrhage or ventricular distention can only be evaluated if the cranial vault is still undamaged. Moreover, it is known that the actual size of cerebrospinal fluid (CSF) spaces is altered by formalin-fixation of the brain [21]. On the other hand, appreciable differences in the ventricular volume between in vivo and postmortem CT studies occurs only after the onset of autolysis.

Since 1980, CT has been performed after fetal or postnatal death in all infants before autopsy in the Department of Neuroradiology, University Hospital, Mainz. We have tried to delineate some aspects of intracranial hemorrhage by comparing postmortem CT and autopsy. Preliminary results have been reported [22].

Received July 15, 1982; accepted after revision September 15, 1982.

Presented at the XII International Symposium Neuroradiologicum, Washington, D.C., October 1982.

[1] Department of Neuroradiology, University Hospital Mainz, Langenbeckstrasse 1, 6500 Mainz, West Germany. Address reprint requests to B. Ludwig.

[2] Department of Pediatric Pathology, University Hospital Mainz, 6500 Mainz, West Germany.

[3] Department of Neuropathology, University Hospital Mainz, 6500 Mainz, West Germany.

[4] Department of Pediatrics, University Hospital Mainz, 6500 Mainz, West Germany.

AJNR **4:27–36, January/February 1983**
0195–6108/83/0401–0027 $00.00
© American Roentgen Ray Society

TABLE 1: **Age Distribution and Type of Hemorrhage of Fetuses and Infants Examined by Postmortem CT and Autopsy**

Type of Hemorrhage: Birth Status	No. Infants (No. Recognized by CT)					
	Gestational Age in Weeks					
	Immature				Mature	Totals
	13–19	20–24	25–29	30–37	38–41	
All infants:						
Stillborn	16	15	5	12	4	52
Died after birth at:						
≤1 week	0	1	8	12	7	28
2–4 weeks	0	0	3	7	3	13
5 weeks–18 months	0	0	2	3	7	12
Totals	16	16	18	34	21	105
Intra-, sub-, or epidural:						
Stillborn	2 (2)	9 (6)	4 (3)	7 (5)	2 (2)	24 (18)
Died after birth at:						
≤1 week	0	1 (1)	4 (2)	7 (3)	3 (1)	15 (7)
2–4 weeks	0	0	1 (1)	4 (3)	0	5 (4)
5 weeks–18 months	0	0	1 (1)	0	2 (1)	3 (2)
Totals	2 (2)	10 (7)	10 (7)	18 (11)	7 (4)	47 (31)
Primary subarachnoid:						
Stillborn	1 (1)	4 (0)	1 (0)	6 (4)	1 (1)	13 (6)
Died after birth at:						
≤1 week	0	0	1 (1)	4 (3)	3 (3)	8 (7)
2–4 weeks	0	0	0	1 (0)	0	1 (0)
5 weeks–18 months	0	0	1 (1)	1 (0)	2 (1)	4 (2)
Totals	1 (1)	4 (0)	3 (2)	12 (7)	6 (5)	26 (15)
Intracerebral:						
Stillborn	4 (4)	4 (3)	2 (1)	1 (0)	0	11 (8)
Died after birth at:						
≤1 week	0	0	5 (3)	5 (5)	1 (1)	11 (9)
2–4 weeks	0	0	3 (2)	3 (1)	2 (1)	8 (4)
5 weeks–18 months	0	0	1 (1)	1 (0)	2 (1)	4 (2)
Totals	4 (4)	4 (3)	11 (7)	10 (6)	5 (3)	34 (23)
Intraventricular:						
Stillborn	2 (2)	5 (5)	3 (3)	0	0	10 (10)
Died after birth at:						
≤1 week	0	0	4 (4)	4 (4)	0	8 (8)
2–4 weeks	0	0	3 (3)	2 (2)	1 (1)	6 (6)
5 weeks–18 months	0	0	1 (1)	0	0	1 (1)
Totals	2 (2)	5 (5)	11 (11)	6 (6)	1 (1)	25 (25)

Materials and Methods

One hundred twenty-five stillborn and deceased live-birth infants (premature or not) were examined by postmortem CT. Subsequent autopsy was refused in eight cases and prevented by maceration in six. Anencephaly was encountered six times. The CT and autopsy findings of the other 105 fetuses and infants form the study material. For this study, gestational age was calculated from the first day of the last menstrual period.

The age of the fetuses and infants ranged from 13 gestational weeks in stillborn infants to 18 postnatal months (table 1). Eighty-four of the neonates were immature (up to 37 weeks gestation) while 21 were mature, reflecting the higher mortality in immaturity. Fifty-two were stillborn; 28 were born live but died in their first week of life; and 13 were born live and died between postnatal weeks 2 and 4. Another 12 infants formed an inhomogeneous group with varying survival times of 5 weeks to 18 months after birth.

The primary causes of death varied with the ages of the fetuses and infants and were not considered in this study.

Cranial CT was performed on an EMI 1010 CT scanner as soon as possible after stillbirth or death. The head was completely examined with paired, 5 mm axial slices parallel to the orbitomeatal lines. At autopsy, the brain was removed as a whole, together with parts of the falx and tentorium, and was fixed by suspension in a 4% buffered formalin solution for 5 days or more before dissection. It was generally sliced into horizontal sections before selecting tissue samples for histology.

Results

Four main sites of intracranial hemorrhage were distinguished: (1) intradural, subdural, or epidural, (2) subarachnoid, (3) intracerebral, and (4) intraventricular. Table 1 lists the different types of hemorrhage as found at autopsy and (in parentheses) as detected by CT.

Intradural, Subdural, or Epidural Hemorrhage

Postmortem pathology: Intradural hemorrhage into the connective tissue of falx, venous sinus wall, or tentorium was encountered commonly at autopsy (47/105 = 45%). Such bleeds were frequently associated with primary sub-

arachnoid hemorrhage (17/47) and intracerebral hematomas (20/47). Intradural hematomas were documented in 17 of the 25 cases with intraventricular hemorrhage, a striking concurrence. The incidence of isolated intradural hemorrhage not associated with other types of intracranial hemorrhage was lower (14/105 = 13%).

Most often, intradural bleeds remained as one or several well defined foci (fig. 1). Sometimes, they occurred as larger layers of bleeding (fig. 2). Less often, these hematomas also involved the subdural space (10/47) or the epidural space (3/47) (fig. 2). Intradural bleeds occurred as often in stillborn (24/52 = 46%) as in live-birth infants (considered as a single group) (23/53 = 43%). However, a lower frequency of intradural bleeding was found in live-birth infants who survived longer. The incidence in immature fetuses and immature infants (40/84 = 48%) was somewhat higher than in the mature infants (7/21 = 33%).

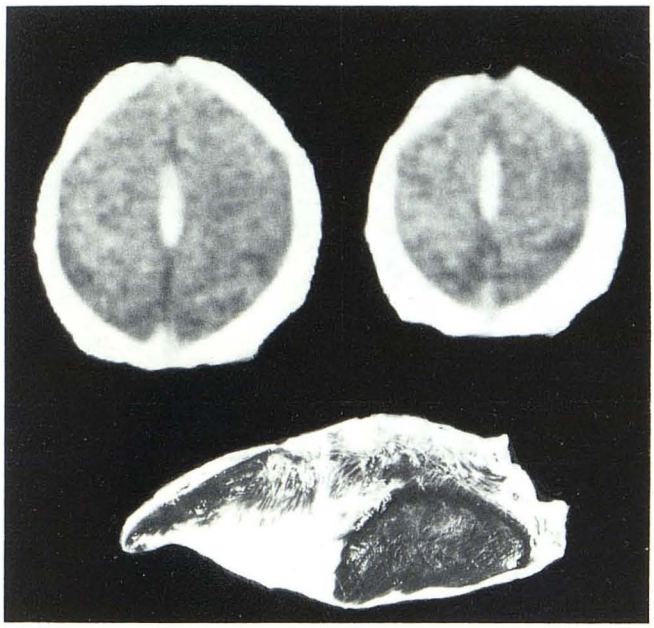

Fig. 1.—Intradural hemorrhage, premature neonate, 32 weeks, birth weight 1,830 g. Death at 2d day of life from complicated delivery and perinatal asphyxia. *CT:* circumscribed hyperdensity in interhemispheric fissure. *Autopsy:* broad intradural hematoma of falx (lateral view).

Postmortem CT: Most (31/47) bleeds observed at postmortem could be correlated with hyperdense structures in the interhemispheric fissure or tentorial region. In the absence of other intracranial hemorrhage, intradural hemorrhage could be recognized in 12 of the 14 cases, depending on the size of the hematomas. However, intradural hemorrhages could not always be identified with certainty by CT alone. Small subdural or epidural hematomas near the falx or tentorium could not be differentiated from intradural hematomas by CT. Antemortem thrombosis of the superior saggittal sinus, occurring once in a preterm neonate of 29 weeks gestation, also mimicked the CT appearance of intradural bleed. In four cases, postmortem clots in bridging veins, sinuses, or deep veins partly or completely mimicked intradural hemorrhage. Because the interhemispheric space is hyperdense in subarachnoid hemorrhage (fig. 3) as well as in intradural hemorrhage, in 12 cases with subarachnoid bleed, the *additional* intradural hematomas in the same region could be detected only at autopsy.

Subarachnoid Hemorrhage

Postmortem pathology: *Primary* subarachnoid hemorrhage from leptomeningeal vessels or bridging veins did not occur more often in any particular patient group. Conversely, nearly all intraventricular hemorrhages (24/25) were accompanied by some bleeding into the subarachnoid spaces that can be assumed to be (at least partially) *secondary* to the initial filling of the ventricles (figs. 4 and 9).

Postmortem CT: Subarachnoid hemorrhage located within the sylvian fissures or the cisterna magna was usually easily detectable (fig. 4), but subarachnoid hemorrhage overlying the convexity was usually overlooked. CT diagnosis of subarachnoid hemorrhage was easier in immature specimens because of the greater width of the external CSF spaces surrounding the brain parenchyma (fig. 4).

Intracerebral Hemorrhage

Postmortem pathology: Intracerebral hematomas were encountered more often in deceased live-birth infants (23/

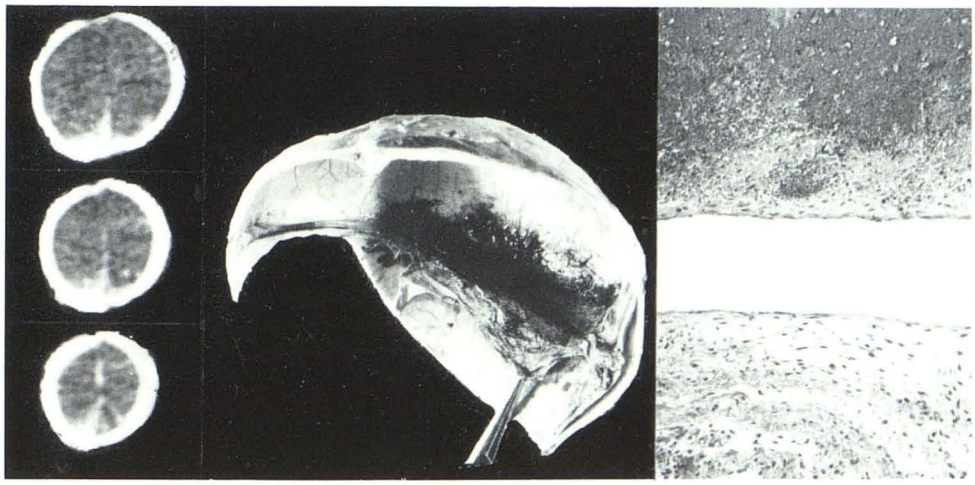

Fig. 2.—Intra-, sub-, and epidural hemorrhage, premature neonate, 31 weeks, birth weight 1,500 g. Death at 1st day of life from consumption coagulopathy after complicated delivery with rupture of liver. *CT:* hyperdensity in the interhemispheric fissure and over adjacent convexity. *Autopsy:* massive intra-, sub-, and epidural hemorrhage (lateral view). *Histology:* intradural hematoma in wall of superior sagittal sinus (*top*), lumen of sinus (*middle*), unaffected contralateral sinus wall (*bottom*).

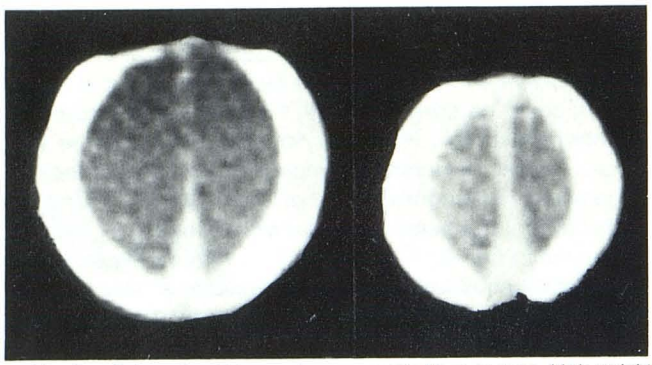

Fig. 3.—Subarachnoid hemorrhage, neonate born at term, birth weight 3,460 g. Death at 1st day of life from perinatal asphyxia and hyaline membrane disease. *CT:* broad hyperdensity in whole interhemispheric fissure. *Autopsy* (not shown): primary subarachnoid hemorrhage.

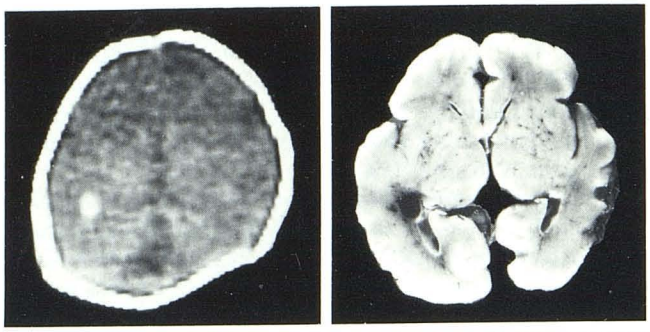

Fig. 5.—Intracerebral hemorrhage, premature neonate, 33 weeks, birth weight 1,420 g. Death at 7th day from respiratory insufficiency caused by cardiac failure. *CT:* left temporooccipital paraventricular hematoma. *Autopsy:* subependymal hematoma without intraventricular hemorrhage.

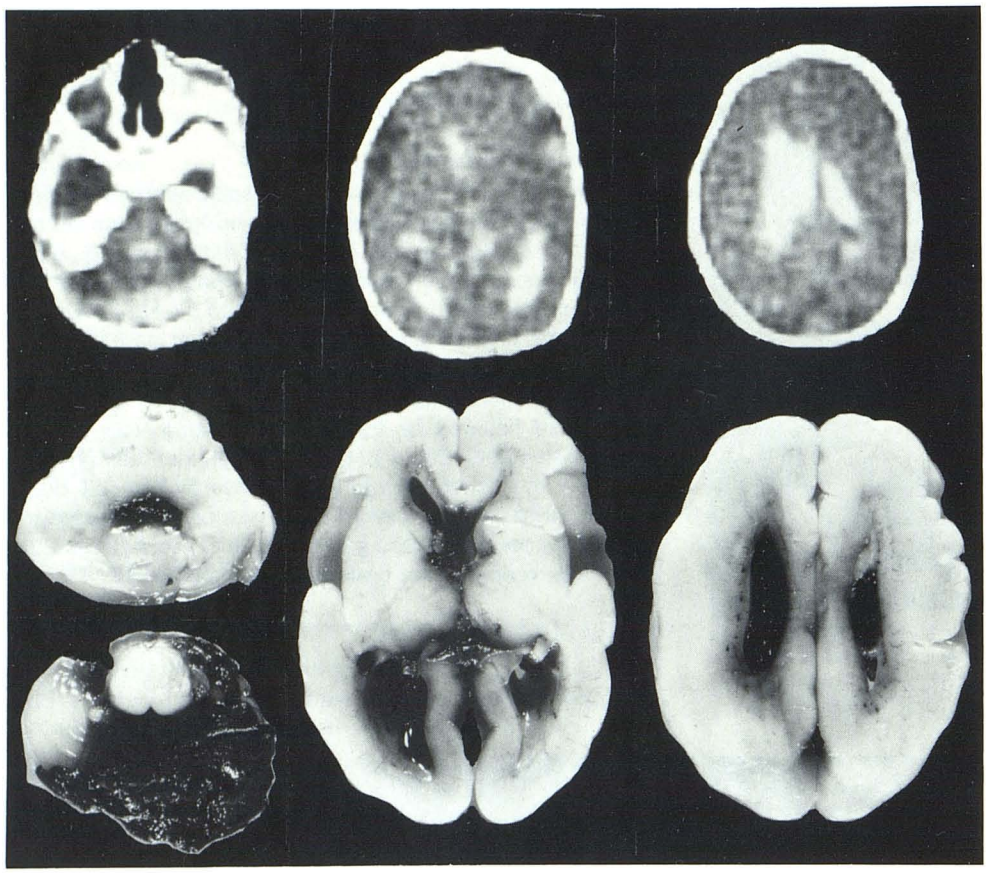

Fig. 4.—Subarachnoid, intracerebral, and intraventricular hemorrhage, stillborn infant, 24 weeks, birth weight 860 g. Interruption after radioiodine treatment in early pregnancy. *CT:* para- and intraventricular hemorrhage, hyperdensity in right sylvian fissure and retrocerebellar subarachnoid space. *Autopsy:* subependymal and intraventricular hemorrhage, secondary subarachnoid hemorrhage.

53 = 43%) than in stillborn infants (11/52 = 21%), and occurred somewhat more often in immature (29/84 = 35%) than in mature infants (5/21 = 24%). Eighteen of the intracerebral hematomas were located subependymally (fig. 5), and seven of the intracerebral hematomas were located in the cortex or the subcortical region. In nine cases, subependymal hemorrhage coexisted with intracerebral hematomas at other sites in the brain parenchyma. Twenty-four of the 34 intracerebral bleeds were associated with intraventricular hemorrhage (figs. 4 and 9). One hematoma in the thalamus was an isolated lesion without any other detectable bleeding site. Intra*cerebellar* hematomas were found in only two cases, both preterm neonates of 29 and 32 weeks, both with multifocal paraventricular hemorrhages.

Postmortem CT: CT and autopsy findings agreed in 23 of the 34 cases of intracerebral hemorrhage. Small subependymal bleeds could be distinguished from the germinal matrix as slightly denser spots in some cases (fig. 6) and occasionally were localized at autopsy only with the aid of

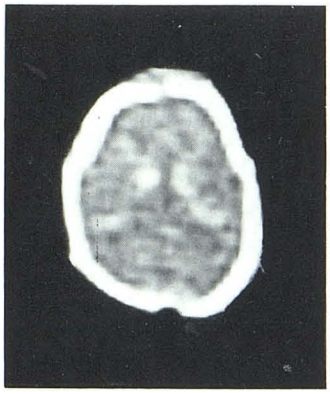

Fig. 6.—Intracerebral hemorrhage, stillborn infant, 19 weeks, birth weight 300 g. Death from placental insufficiency. *CT:* focal paraventricular hyperdensity (46–48 Hounsfield units [H]) within less hyperdense (33–36 H) germinal matrix of left frontal region. (*Autopsy:* [not shown]: subependymal hematoma without intraventricular hemorrhage.) Physiologically large ventricles surrounded by matrix not clearly demonstrated because attenuation difference between CSF and immature white matter is too small at this age.

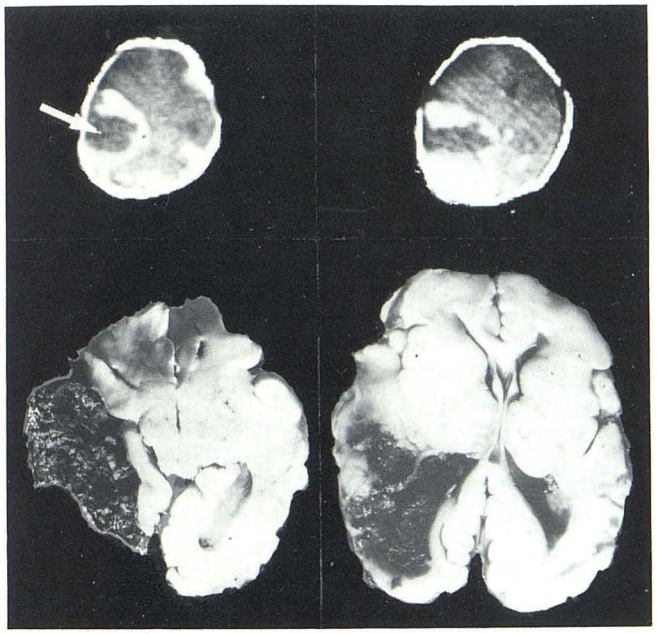

Fig. 7.—Subarachnoid, intracerebral, and intraventricular hemorrhage, hemorrhagic infarction, premature neonate, 36 weeks, birth weight 1,700 g. Death at 8th day from hyaline membrane disease and pneumonia. *CT:* subarachnoid, para-, and intraventricular hemorrhage. In left temporooccipital region, large intracerebral hemorrhage with central hypodense area (*arrow*). *Autopsy:* subependymal and intraventricular hemorrhage, secondary subarachnoid bleed. Left temporooccipital hemorrhagic infarction communicating with occipital horn.

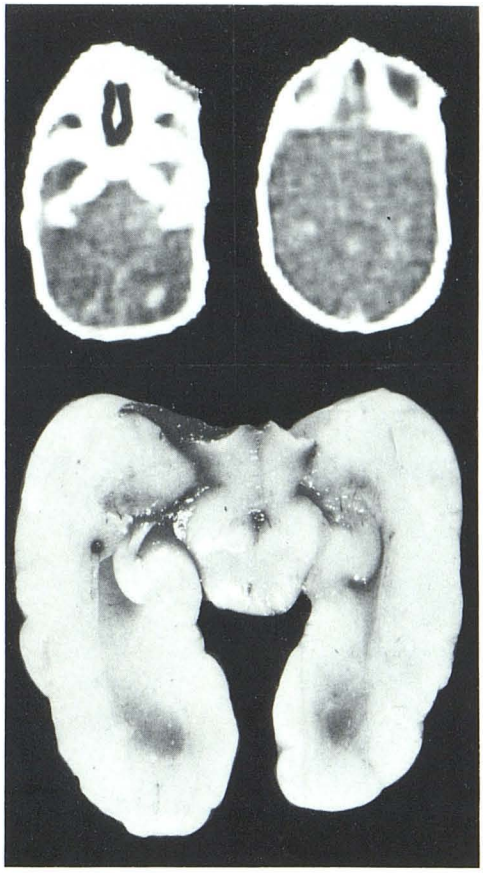

Fig. 8.—Subependymal and intraventricular hemorrhage, premature neonate, 27 weeks, birth weight 620 g. Death at 4th day from perinatal asphyxia caused by immaturity. *CT:* small left temporooccipital paraventricular hematoma, slight intraventricular hemorrhage in occipital horns. *Autopsy:* small subependymal hematoma. Rupture of ependyma, but no detectable intraventricular hemorrhage.

CT. However, distinction of hemorrhage from normal germinal matrix may be extremely difficult. Most of the 11 min hematomas that were overlooked were located in the physiologically hyperdense germinal matrix of the immature brain. Conversely, in two cases, the opacities of the germinal matrix above the head of the caudate nucleus were misdiagnosed as subependymal hematomas. Less often, hyperdensities within or outside the periventricular region represented hemorrhagic infarcts (fig. 7).

Intraventricular Hemorrhage

Postmortem pathology: Intraventricular hemorrhage was rare in those specimens of *mature* stillborn infants or deceased live-birth infants (1/21 = 5%). During *immaturity*, intraventricular hemorrhage occurred more often in the group of live-birth infants (14/36 = 39%) than in the stillborn infants (10/48 = 21%). Of the 25 intraventricular hemorrhages, 21 were associated with subependymal hematomas mostly communicating with the ventricles. In two stillborn infants at 20 and 28 weeks with small intraventricular bleeds, no associated intracerebral hemorrhage could be detected. One of these also showed hemorrhage in the choroid plexus that might be considered the bleeding source.

Postmortem CT: Intraventricular hemorrhage was detected by CT in all cases, sometimes as a small sediment of blood in the occipital horns (fig. 8). The amount of blood within the ventricles and the degree of ventricular dilatation could be calculated better by CT (figs. 4 and 9–11). The precise site of ependymal rupture and bleeding site were identified better by pathologic examination. In two cases, the CT findings of minimal intraventricular hemorrhage could

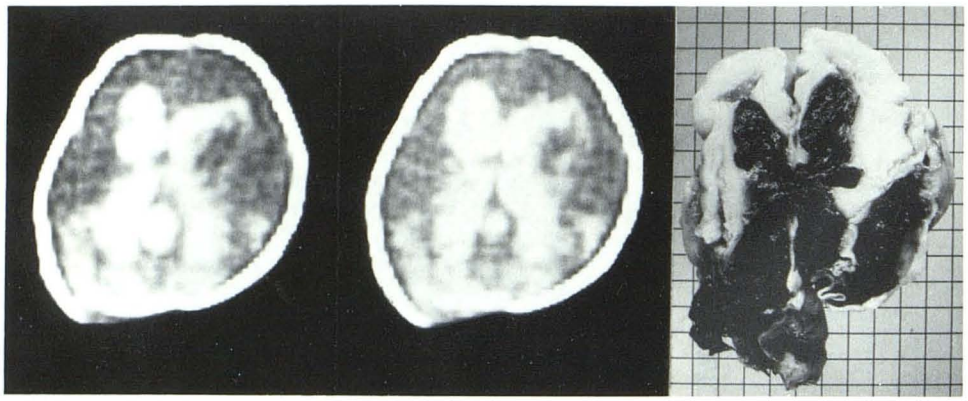

Fig. 9.—Intraventricular, periventricular, and subarachnoid hemorrhage, premature neonate, 29 weeks, birth weight 1150 g. Death at 33d day of life from hyaline membrane disease, renal insufficiency, and enterocolitis. *CT:* massive intraventricular hemorrhage with several paraventricular hematomas, subarachnoid hemorrhage. *Autopsy:* subependymal and large intracerebral hematomas without and with communication with ventricular system (latter partly representing bleeding source, partly caused by bursting of ventricles), intraventricular hemorrhage with tamponade of ventricles, secondary subarachnoid hemorrhage.

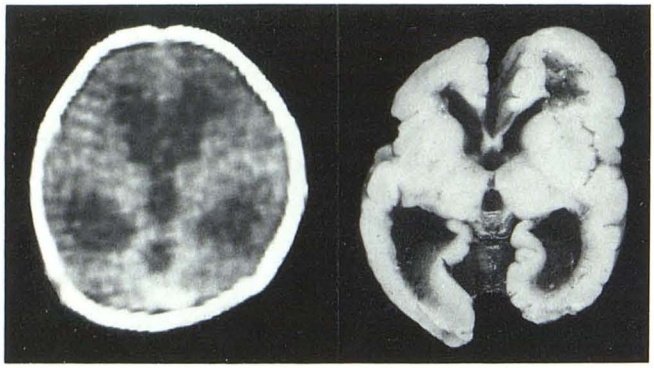

Fig. 10.—Hydrocephalus after intracranial hemorrhage, premature neonate, 29 weeks, birth weight 1,510 g. Death at 25th day from hyaline membrane disease. *CT:* enlargement of ventricular system, periventricular lucency, slight deformation of right frontal horn. *Autopsy:* posthemorrhagic hydrocephalus after intraventricular and secondary subarachnoid hemorrhage, partly resorbed right frontal intracerebral hematoma communicating with ventricle.

not be verified at autopsy, presumably because the blood-stained CSF was lost in removing the brain. However, the existence of prior intraventricular hemorrhage could be suggested by ependymal defects at the margin of paraventricular hematomas (fig. 8).

The subependymal germinal matrix, which forms bilateral hyperdense layers beside the lateral ventricles in the immature brain, can be confused with intraventricular hemorrhage (fig. 12). However, the slight differences in density between germinal matrix and hemorrhage or the more lateral distribution of the matrix permitted correct diagnosis in all cases.

Discussion

A prior study of in vivo CT examinations of full-term neonates [7] documented the presence of hyperdense structures in the interhemispheric fissure and in the region of the tentorium cerebelli. These structures could be seen as isolated findings in 27 (18%) of 150 neonates and in 58% of neonates with other types of intracranial hemorrhage. The question of whether these findings actually represent (1) suspected intradural or subdural bleeds, (2) physiologic structures (e.g., the sinuses or the falx), or (3) similarly appearing interhemispheric and juxtatentorial subarachnoid hemorrhage [20, 23–27] remained unresolved in most cases because of the low mortality in the examined group. On the basis of the present study, we conclude that comparable changes in postmortem CT scans nearly always proved to be hemorrhages at autopsy and that most of such interhemispheric and juxtatentorial hemorrhages proved to be located intradurally.

Intradural bleeds in the falx or the tentorium may appear isolated, disseminated, or confluent. Their preferred areas are the wall or the surroundings of the superior sagittal sinus. Intradural hemorrhage is usually considered traumatic [28–30]. The high incidence in the immature group (48%) might be consistent with this hypothesis, because, in preterm delivery, the infantile skull is compressed and deformed considerably within the rigid cervix [31]. Moreover, the connective tissue of the immature falx is looser and more vulnerable than in full-term neonates.

On the other hand, hematomas with histopathologically proven cellular reaction of the surrounding tissue cannot result from birth trauma in babies dying during or soon after delivery. Indeed, we have seen these bleeds in some fetuses who died in utero a few days before the onset of labor. In such cases, the intradural hemorrhage may be related to intrauterine asphyxia. We have also detected intradural hematomas in association with most intraventricular bleeds, which are regarded as being predominantly hypoxic in origin [30, 32–36]. The possibility that many of the intradural hematomas are of hypoxic origin has been discussed by Friede [28].

In agreement with Friede [28], we do not think that the intradural bleeds per se are of clinical significance. Even large confluent hematomas (fig. 1) did not have a thickness more than 2–3 mm and, thus, did barely develop any significant space-occupying effect onto the brain. However, intradural hemorrhage may indicate prior mechanical or ischemic injury to the brain. In accord with this concept, our earlier study [7] demonstrated few neurologic signs in most full-term neonates with hyperdense structures believed to be intradural bleeds, who otherwise had normal CT scans. This group had a good prognosis in radiologic as well as clinical follow-up examinations [12], consistent with the fact

Fig. 11.—Hydrocephalus after intracranial hemorrhage, premature neonate, 31 weeks, birth weight 1300 g. Death at 36th day from perinatal sepsis and severe posthemorrhagic hydrocephalus. *CT:* enlargement of ventricular system, periventricular lucency, and more distinct right frontal hypodensity. *Autopsy:* posthemorrhagic hydrocephalus after recurrent intraventricular and subarachnoid hemorrhage, large right frontal bleeding cavity communicating with ventricle.

that within a few months after birth, organized hematomas or pigmentation in falx or tentorium can be found only sporadically [28].

In contrast to intradural hemorrhage, *subdural* hematomas in the neonatal period have received wide recognition and have been reported in large autopsy series [36–38] and CT studies [17, 39]. Subdural hemorrhage may result from mechanical injuries, for example, tearing of bridging veins or lacerations of tentorium, falx, or large venous channels [29, 31, 40, 41]. In our series, however, we never observed tentorial or falcine lacerations. We group the subdural hematomas with the intradural bleeds because they seemed to be part of a primary multicentric hemorrhage in the falcine or tentorial area. They did not appear to result from rupture of substantial intradural hematomas into the subdural space.

The high frequency of tentorial or falcine lacerations and of subdural hematomas in some older autopsy studies [29, 40, 41] may be explained partly by confusion with intradural bleeds or asphyxial hemorrhage and partly by interim improvement in obstetrical management [28, 31]. Recently, Friede [28] found very few dural lacerations in his autopsies. Larroche [38] reviewed 700 autopsies and detected subdural bleeds in 18% of term and 11% of preterm infants who died. The incidence of subdural hematomas in our postmortem examinations was 10 (9.5%) of 105.

Diffuse primary *subarachnoid* hemorrhage (not secondary spread from intraventricular bleed by leakage through the foramina of the fourth ventricle) is usually regarded as hypoxic in origin [38]. Traumatic rupture of bridging veins within the subarachnoid space may be another source of subarachnoid hemorrhage [31, 42]. Subarachnoid bleed located only over the convexity may be caused by consumptive coagulopathy [43].

We detected subarachnoid hemorrhage in fetuses and infants of varying degrees of maturity and viability (table 1). Radiologically, the hemorrhage has been detected most easily in the sylvian fissures by CT. Localized subarachnoid bleeds over the temporal or occipital lobes or along the basal cerebellar surfaces were frequently observed at autopsy but proved to be difficult to differentiate from the adjacent skull radiologically and, thus, were mostly overlooked by CT.

The incidence and primary locus of *intracerebral* hematoma varies with the degree of brain maturity [17, 31]. The periventricular germinal matrix is the typical bleeding site of spontaneous hypoxic hemorrhage in the immature brain (fig. 13) [35, 44–46]. The matrix is an infrequent site of hemorrhage in full-term neonates [7, 17, 47]. Subependymal bleeds develop most often within the first days of life [48, 49]. They are the main source of *intraventricular* hemorrhage (which was also most common in the immature neonates in our postmortem study). The choroid plexus appeared to be the primary source of intraventricular hemorrhage [50] in only one immature stillborn infant. Infrequently, paraventricular hematomas with multilocular distribution have been caused by bursting of the ventricular walls after tamponade of the ventricles (fig. 9) [1, 51]. Large hemorrhagic cavities that arise during resorption of paraventricular hematomas may be overlooked by CT when their content is still isodense with brain (fig. 10). Such cavities become visible when they achieve their final hypodensity (fig. 11).

Infarctions with secondary development of hemorrhage within the necrotic tissue [52] were found in or distant from the periventricular region. They were always combined with other intracerebral or intraventricular bleeds. By CT alone, hemorrhagic infarctions could not be distinguished from

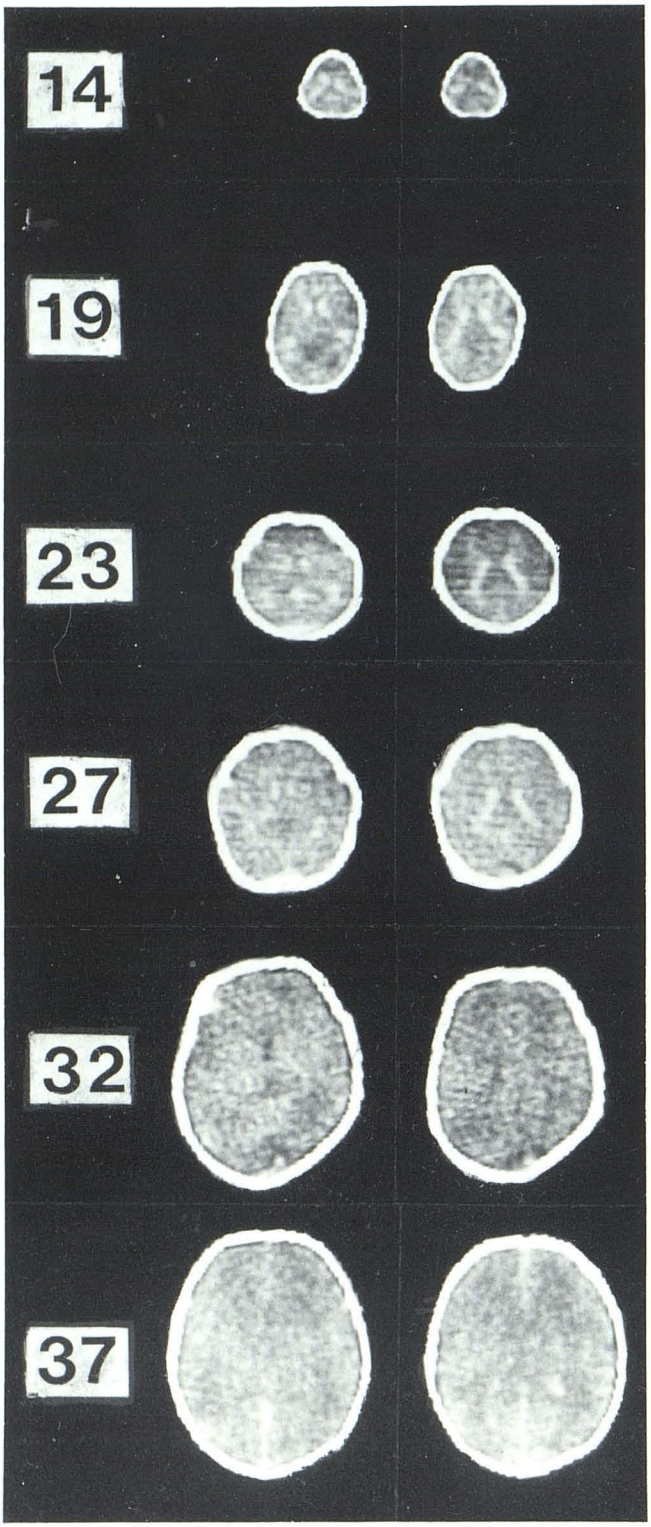

Fig. 12.—Development of periventricular germinal matrix, stillborn infants at 14–37 weeks without para- or intraventricular hemorrhage. Symmetric hyperdense layers surrounding lateral ventricles decrease in thickness and attenuation up to 27 weeks and cannot be detected in stillborns at 32–37 weeks.

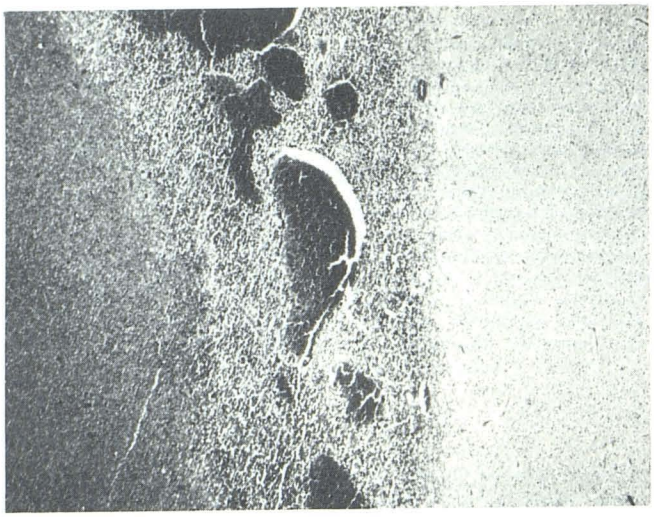

Fig. 13.—Hematoma in germinal matrix, premature neonate, 32 weeks, birth weight 1,800 g, death at 2d day of life. Histologic section of subependymal hematoma communicating with ventricle (*left*), normal matrix tissue with congested vessels (*middle*), and cerebral parenchyma (*right*).

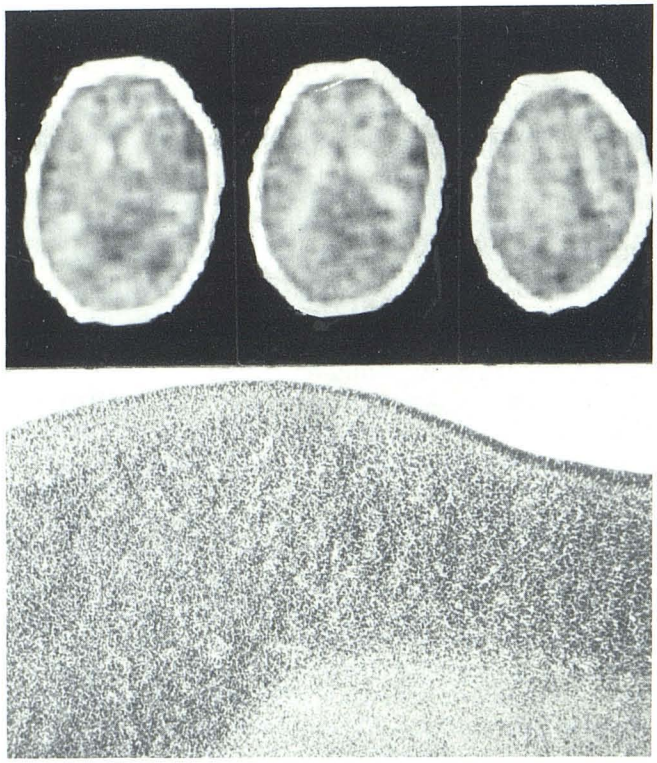

Fig. 14.—Normal germinal matrix, stillborn infant, 19 weeks, birth weight 340 g, death from amnionitis. *CT:* normal paraventricular hyperdensity of germinal layer. *Histology:* normal appearance of ependyma (*top*), germinal matrix (*middle*), and brain parenchyma (*bottom*).

hematomas unless their hyperdensities were accompanied by low-density areas. The latter had, however, to be located not only at the margin of the bleed (in distinction from a partially resorbed hematoma) (fig. 7).

In evaluating the CT scans of immature brains, the *physiological hyperdensity of the subependymal germinal layer,*

or matrix, must be considered [16, 20, 22, 53]. Histologically, the matrix tissue is characterized by tightly packed immature cells, a picture sometimes resembling lymphoid tissue. The density of cells, rather than the marked vascularity of this area is reponsible for the hyperdensity observed by CT (figs. 13 and 14).

The germinal matrix completely surrounds the lateral ventricles up to the 30 weeks gestation (fig. 12). It is most prominent along the thalamocaudate groove and above the head of the caudate nucleus [28, 38].

On CT, the symmetric juxtaventricular matrix may be mistaken for hemorrhage within the lateral ventricles. Another explanation for this erroneous diagnosis results from difficulties in outlining the ventricles. The physiologically large ventricular cavities of the immature brain decrease gradually during the intrauterine development until they are slitlike in most term neonates and may be overlooked on CT. Moreover, the outlines of the ventricles are poorly defined because the attenuation difference between the CSF and the low cell density of the adjacent frontal and temporooccipital white matter is still small in the immature brain [20, 28].

The matrix tissue persists as scattered paraventricular islands during the last weeks of gestation and sometimes even in full-term neonates. If these focal residues of the matrix between the caudate nucleus and the thalamus are large enough to be detected by CT, they are easily confused with subependymal hematomas. On the other hand, if the early linear or the late focal paraventricular hyperdense pattern is slightly asymmetric in shape or in attenuation on CT (fig. 6), subependymal hemorrhage should be suspected [16, 22].

REFERENCES

1. Burstein J, Papile LA, Burstein R. Subependymal germinal matrix and intraventricular hemorrhage in premature infants: diagnosis by CT. *AJR* **1977**;128:971–976
2. Dittrich M, Ludwig B, Brand M, Dinkel E. Stellenwert der sonographischen Zerebraldiagnostik bei Risikoneugeborenen. Ein Vergleich mit der Computertomographie. Presented at the international Berlin meeting of perinatal medicine, Berlin, December **1981**
3. Flodmark O, Fitz CR, Harwood-Nash DC. The CT diagnosis and short term prognosis of intracranial hemorrhage and hypoxic/ischemic brain damage in neonates. *J Comput Assist Tomogr* **1980**;4:775–787
4. Grant EG, Borts FT, Schellinger D, McCullough DC, Sivasubramanian KN, Smith J. Real-time ultrasonography of neonatal intraventricular hemorrhage and comparison with computed tomography. *Radiology* **1980**;139:667–691
5. Krishnamoorthy KS, Fernandez RA, Momose KJ, et al. Evaluation of neonatal intracranial hemorrhage by computerized tomography. *Pediatrics* **1977**;59:165–172
6. Lee BCP, Grassi AE, Schechner S, Auld PAM. Neonatal intraventricular hemorrhage: a serial computed tomography study. *J Comput Assist Tomogr* **1979**;3:483–490
7. Ludwig B, Brand M, Brockerhoff P. Postpartum CT examination of the heads of full term infants. *Neuroradiology* **1980**;20:145–154
8. Rumack CM, McDonald MM, O'Meara OP, Sanders BB, Rudikoff JC. CT detection and course of intracranial hemorrhage in premature infants. *AJR* **1978**;131:493–497
9. Sauerbrei EE, Digney M, Harrison PB, Cooperberg PL. Ultrasonic evaluation of neonatal intracranial hemorrhage and its complications. *Radiology* **1981**;139:677–685
10. Scott WR, New PFJ, Davis KR, Schnur JA. Computerized axial tomography of intracerebral and intraventricular hemorrhage. *Radiology* **1974**;112:73–80
11. Albright L, Fellows R. Sequential CT scanning after neonatal intracerebral hemorrhage. *AJNR* **1981**;2:133–137, *AJR* **1981**;136:949–953
12. Brand M, Ludwig B. Die Prognose intracranieller Blutungen bei Neugeborenen (Nachuntersuchungen bis zum 3. Lebensjahr). Presented at the Tagung der Deutschen Gesellschaft für Kinderheilkunde, Düsseldorf, September **1981**
13. Burstein J, Papile LA, Burstein R. Intraventricular hemorrhage and hydrocephalus in premature newborns: a prospective study with CT. *AJR* **1979**;132:631–635
14. Flodmark O, Scotti G, Harwood-Nash DC. Clinical significance of ventriculomegaly in children who suffered perinatal asphyxia with or without intracranial hemorrhage: an 18 month follow-up study. *J Comput Assist Tomogr* **1981**;5:663–673
15. Schrumpf JD, Sehring S, Killpack S, Brady JP, Hirata T, Mednick JP. Correlation of early neurological outcome and CT findings in neonatal brain hypoxia and injury. *J Comput Assist Tomogr* **1980**;4:445–450
16. Fitz CR, Martin DJ, Pape K, Chuang SH. Phantom hematomas—the misinterpretation of normal germinal matrix as subependymal hemorrhage. Presented at the annual meeting of the Society for Pediatric Radiology, San Francisco, March **1981**
17. Flodmark O, Becker LE, Harwood-Nash DC, Fitzhardinge PM, Fitz CR, Chuang SH. Correlation between computed tomography and autopsy in premature and full-term neonates that have suffered perinatal asphyxia. *Radiology* **1980**;137:93–103
18. Oldendorf WH. Some possible applications of computerized tomography in pathology. *J Comput Assist Tomogr* **1980**;4:141–144
19. Pevsner PH, Garcia-Bunuel R, Leeds N, Finkelstein M. Subependymal and intraventricular hemorrhage in neonates. *Radiology* **1976**;119:111–114
20. Picard L, Claudon M, Roland J, et al. Cerebral computed tomography in premature infants, with an attempt at staging development features. *J Comput Assist Tomogr* **1980**;4:435–444
21. Sarwar M, McCormick WF. Decrease in ventricular and sulcal size after death. *Radiology* **1978**;127:409–411
22. Ludwig B, Becker K, Bohl J. Postmortale Computertomographie und Autopsie bei perinatalen intrakraniellen Blutungen. Presented at the Jahrestagung der Deutschen Gesellschaft für Neuroradiologie, Tübingen, W. Germany, October **1981**
23. Dolinskas CA, Zimmerman RA, Bilaniuk LT. A sign of subarachnoid bleeding on cranial computed tomograms of pediatric head trauma patients. *Radiology* **1978**;126:409–411
24. Lim ST, Sage DJ. Detection of subarachnoid blood clot and other thin, flat structures by computed tomography. *Radiology* **1977**;123:79–84
25. New PFJ, Aronow S. Attenuation measurements of whole blood and blood fractions in computed tomography. *Radiology* **1976**;121:635–640
26. Norman D, Price D, Boyd D, et al. Quantitative aspects of computed tomography of the blood and cerebrospinal fluid. *Radiology* **1977**;123:335–338
27. Osborn AG, Anderson RE, Wing SD. The false falx sign. *Radiology* **1980**;134:421–425

28. Friede RL. *Developmental neuropathology.* Vienna, Austria: Springer, **1975**
29. Pott R. Über Tentoriumzerreissungen bei der Geburt. *Z Geburtshilfe Perinatol* **1911**;69:674–718
30. Ylppö A. Pathologisch-anatomische Studien bei Frühgeborenen. *Eur J Pediatr* **1919**;20:212–431
31. Pape KE, Wigglesworth JS. *Hemorrhage, ischaemia and the perinatal brain.* London: Heinemann, **1979**
32. Fedrick J, Butler NR. Certain causes of neonatal death. II. Intraventricular haemorrhage. *Biol Neonate* **1971**;15:157–290
33. Harcke HT Jr, Naeye AL, Storch A, Blanc WA. Perinatal cerebral intraventricular hemorrhage. *J Pediatr* **1972**;80:37–42
34. Leech RW, Kohnen P. Subependymal and intraventricular hemorrhages in the newborn. *Am J Pathol* **1974**;77:465–475
35. Towbin A. Cerebral intraventricular hemorrhage and subependymal matrix infarction in the fetus and premature newborn. *Am J Pathol* **1968**;52:121–123
36. Valdes-Dapena MA, Arey JB. The causes of neonatal mortality: an analysis of 501 autopsies on newborn infants. *J Pediatr* **1970**;77:366–375
37. Fedrick J, Butler NR. Certain causes of neonatal death. V. Cerebral birth trauma. *Biol Neonate* **1971**;18:321–329
38. Larroche JC. *Developmental pathology of the neonate.* Amsterdam: Excerpta Medica, **1977**
39. Zimmerman RA, Bilaniuk LT, Bruce D, Schut L, Uzzel B, Goldberg HI. Interhemispheric acute subdural hematoma: a computed tomographic manifestation of child abuse by shaking. *Neuroradiolgy* **1978**;16:39–40
40. Holland E. On cranial stress in the foetus during labour and on the effects of excessive stress on the intracranial contents; with an analysis of eighty-one cases of torn tentorium cerebelli and subdural cerebral hemorrhage. *Trans Edinb Obstet Soc* **1921**;40:112–143
41. Beneke R. Über Tentoriumzerreissungen bei der Geburt sowie die Bedeutung der Duraspannung für chronische Gehirnerkrankungen. *Munch Med Wochenschr* **1910**;57:2125–2127
42. Towbin A. Central nervous system damage in the human fetus and newborn infant. Mechanical and hypoxic injury incurred in the fetal-neonatal period. *Am J Dis Child* **1970**;119:529–542
43. Chessels JM, Wigglesworth JS. Secondary haemorrhagic disease of the newborn. *Arch Dis Child* **1970**;45:539–543
44. Deonna T, Payot M, Probst A, Prod'hom LS. Neonatal intracranial hemorrhage in premature infants. *Pediatrics* **1975**;56:1056–1064
45. Gruenwald P. Subependymal cerebral hemorrhage in premature infants and its relation to various injurious influences at birth. *Am J Obstet Gynecol* **1951**;61:1285–1292
46. Volpe JJ. Neonatal intracranial hemorrhage. Pathophysiology, neuropathology, and clinical features. *Clin Perinatol* **1977**;4:77–102
47. Palma PA, Miner ME, Morris FH, Adcock III EW, Denson SE. Intraventricular hemorrhage in the neonate born at term. *Am J Dis Child* **1979**;133:941–944
48. Dyer NC, Brill AB, Tsiantos AC, Sell E, Victorin LH, Stahlman MT. Timing of intracranial bleeding in newborn infants. *J Nucl Med* **1973**;14:807–811
49. Tsiantos A, Victorin L, Reiler JP, et al. Intracranial hemorrhage in the prematurely born infant: timing of clots and evaluation of clinical signs and symptoms. *J Pediatr* **1974**;85:854–859
50. Donat JF, Okazaki H, Kleinberg F, Reagan TJ. Intraventricular hemorrhages in full-term and premature infants. *Mayo Clin Proc* **1978**;53:437–441
51. Rydberg E. Cerebral injury in newborn children consequent on birth injury. *Acta Pathol Microbiol Scand* **1932**;[Suppl 10]:1–247
52. Armstrong D, Norman MG. Periventricular leucomalacia in neonates: complications and sequelae. *Arch Dis Child* **1974**;49:367–375
53. Larroche JC. Critères morphologiques du développement du système nerveux central du foetus humain. *J Neuroradiol* **1981**;8:93–108